Counteracting sensitivity accumulation near source and receiver locations in 3-D inversion of controlled-source electromagnetic data

Paula Rulff[1], Thomas Kalscheuer[1], Dominik Zbinden[formerly at 1] | [1]Dept. of Earth Sciences, Uppsala University, Sweden | **paula.rulff@geo.uu.se**

EGU23-5006 @EMRP2.12

This presentation participates in OSPP
Outstanding Student & PhD candidate Presentation contest

1. Introduction & Objectives

- synthetic controlled-source electromagnetic (CSEM) inversion study with a single transmitter and a distant inclined conductive anomaly ⇒ mitigate the influence of strong sensitivities near source and receivers
- 3-D CSEM finite-element approximations [1,2] combined with non-linear conjugate gradient (NLCG) inversion [3] implemented in inversion framework [4] ⇒ guide the inversion to a reliable model via the model regularisation term

How can we prevent resistivity artefacts close to the source location?

2. Study

Model

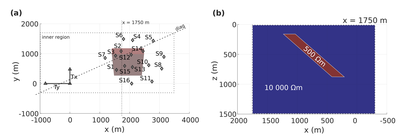

Figure 1: (a) Top view on measurement set-up with locations of the block anomaly. (b) Vertical section through the inner model region displaying the true model resistivities.

Data

- 11 frequencies (10^2 - 10^4 Hz)
- Zxy & Zyx with 2 % noise
- Zxx & Zyy with abs. error of Zxy & Zyx

Inversion settings

- 30 iterations
- 10 000 Ωm start model
- sources & receivers in thin fixed layer
- 67 663 free model parameters

Tests

- preconditioning
- impedance components
- regularisation weights

Data gradients

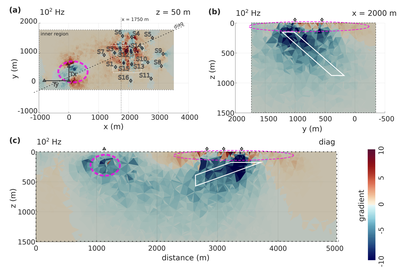

Figure 2: Sections through the inner model region displaying gradients at 10^2 Hz of Zxy & Zyx data. The location of the conductive anomaly is outlined in white. Areas of high sensitivities near source and receivers are outlined in pink. Mesh: tetgen [5]

3. Results

Zxy & Zyx input data

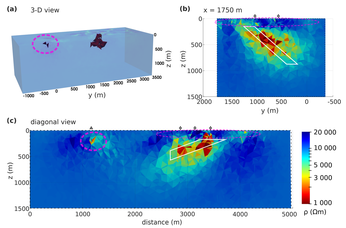

Figure 3: (a) 3-D view and (b,c) vertical sections through the resistivity model obtained with preconditioned NLCG inversion and Zxy & Zyx input data. ρ-threshold in (a): 1 000 Ωm.

Full Z input data

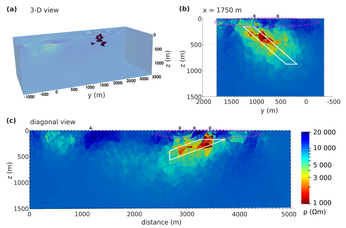

Figure 4: (a) 3-D view and (b,c) vertical sections through the resistivity model obtained with preconditioned NLCG inversion and all Z components as input data.

Zxy & Zyx input data with distance-to-source weights

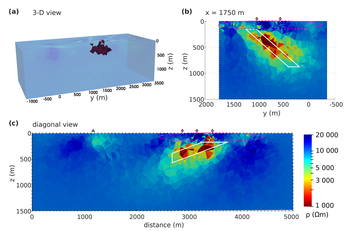

Figure 5: (a) 3-D view and (b,c) vertical sections through the resistivity model obtained with preconditioned NLCG inversion and distance-to-source weights ($r_d = 750\ m$).

Analysis

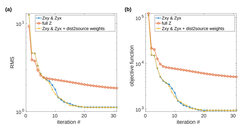

Figure 6: Convergence analysis: (a) RMS and (b) objective function versus iteration number.

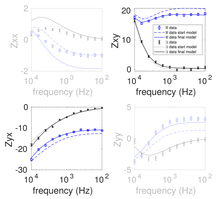

Figure 7: Data-fit S1 with distance-to-source weights.

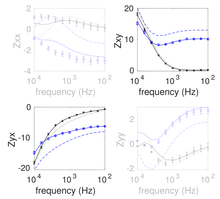

Figure 8: Data-fit S14 with distance-to-source weights.

Take-aways

⇒ It is difficult to remove the source signature in the resistivity model, but possible to reduce artefacts by increasing the smoothing in the source region.

⇒ Diagonal components of the impedance tensor add information, but are more difficult to fit than off-diagonal components.

⇒ Do not place the transmitter above known resistivity anomalies!

CSEM Impedance Tensor Z

- "Controlled-source tensor magnetotellurics" [9,10]
- impedance tensor **Z** defined via horizontal electric and magnetic fields
- two independent source polarisations (subscripts 1 & 2)
- source current does not need to be known

$$Z_{xx} = \frac{E_{x1}H_{y2} - E_{x2}H_{y1}}{H_{x1}H_{y2} - H_{x2}H_{y1}}, \quad Z_{xy} = \frac{E_{x2}H_{x1} - E_{x1}H_{x2}}{H_{x1}H_{y2} - H_{x2}H_{y1}},$$
$$Z_{yx} = \frac{E_{y1}H_{y2} - E_{y2}H_{y1}}{H_{x1}H_{y2} - H_{x2}H_{y1}}, \quad Z_{yy} = \frac{E_{y2}H_{x1} - E_{y1}H_{x2}}{H_{x1}H_{y2} - H_{x2}H_{y1}}.$$

4. Methods

Distance-to-source (r) weights

- weights $w_i(r)$ in the model regularisation term
- increase the smoothing in model regions, where sensitivities are high, but no variations in subsurface resistivity are expected (at source location)

$$w_i(r) = \begin{cases} \left(\frac{r_i}{r_d}\right)^{-3} & \text{for} \quad r_i \leq r_d; \\ 1 & \text{for} \quad r_i > r_d. \end{cases}$$

- for first-order difference regularisation [7] and gradient approximation via the weighted sum of first differences [8]

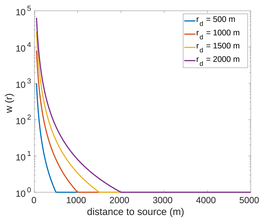

Figure 9: weights $w_i(r)$

Preconditioning

- approximates the Hessian of the objective function Φ
- distributes the model update $\mathbf{m}_{k+1}$ more uniformly in the domain due to better search directions $\mathbf{u}_k$

Preconditioner suggested in [6] with step size α_k:

$$\mathbf{M}_{k+1} = \mathbf{M}_k + \frac{\nabla\Phi(\mathbf{m}_k)\nabla\Phi(\mathbf{m}_k)^T}{\nabla\Phi(\mathbf{m}_k)^T\mathbf{u}_k} + \frac{\mathbf{v}_k\mathbf{v}_k^T}{\alpha_k\mathbf{v}_k^T\mathbf{u}_k}$$

- diagonal preconditioner updated at each iteration k
- $\mathbf{M}_0$ is set to the identity matrix, $\mathbf{v}_k = \nabla\Phi(\mathbf{m}_{k+1}) - \nabla\Phi(\mathbf{m}_k)$

References

[1] J. Jin. The Finite Element Method in Electromagnetics. Wiley-IEE Press, 3th edition, 2014.
[2] Rulff, P., Buntin, L. M. and Kalscheuer, T. (2021) Efficient goal-oriented mesh refinement in 3-D finite-element modelling adapted for controlled source electromagnetic surveys. Geoph. J. Int., 227, 1624–1645.
[3] Zbinden, D. (2015) Inversion of 2D Magnetotelluric and Radiomagnetotelluric Data with Non-Linear Conjugate Gradient Techniques. Thesis, Uppsala University.
[4] T. Kalscheuer, M. d. l. A. Garcia Juanatey, N. Meqbel, L. B. Pedersen. Non-linear model error and resolution properties from two-dimensional single and joint inversions of direct current resistivity and radiomagnetotelluric data. Geophys. J. Int., 182(3):1174-1188, 2010.
[5] Hang Si. TetGen, a Delaunay-Based Quality Tetrahedral Mesh Generator. ACM Trans. on Mathematical Software. 41(2), Article 11 (February 2015), 2015.
[6] Newman, G. A. and Alumbaugh, D. L. (2000) Three-dimensional magnetotelluric inversion using non-linear conjugate gradients. Geoph. J. Int., 140, 410–424.
[7] Rücker, C. (2011) Advanced Electrical Resistivity Modelling and Inversion using Unstructured Discretization. Ph.D. thesis, University of Leipzig.
[8] Key, K. (2016) MARE2DEM: A 2-D inversion code for controlled-source electromagnetic and magnetotelluric data. Geoph. J. Int., 207, 571–588.
[9] Li, X. and Pedersen, L. B. (1991) Controlled source tensor magnetotellurics. Geoph., 56, 1456–1461.
[10] Bretaudeau, F. and Coppo, N. (2016) A pseudo-MT formulation for 3D CSEM inversion with a single transmitter. Conference Paper at EMIW2016.

UPPSALA UNIVERSITET

The computations were enabled by resources provided by the National Academic Infrastructure for Supercomputing in Sweden (NAISS) at UPPMAX (SNIC 2022/5-530) partially funded by the Swedish Research Council (2022-06725).

This work was partly funded by the Smart Exploration project. Smart Exploration has received funding from the European Union's Horizon 2020 research and innovation programme under grant agreement No. 775971.

linkedin.com/in/paula-rulff
@emgeopaula